AD-A191 045 CORROSION OF ELECTROLESS NICKEL-COATED STEEL(U) NAVAL SURFACE WEAPONS CENTER SILVER SPRING MD J F MCINTYRE ET AL. 01 APR 87 NSWC/TR-87-170 1/1

UNCLASSIFIED F/G 11/3 NL

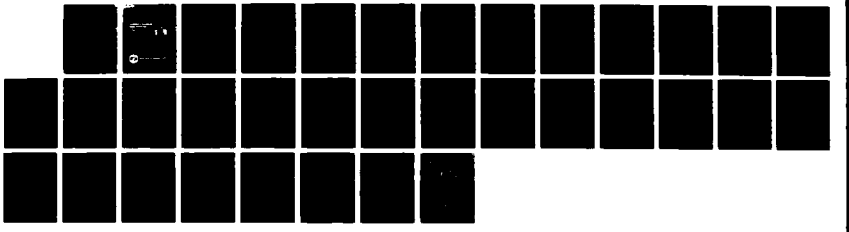

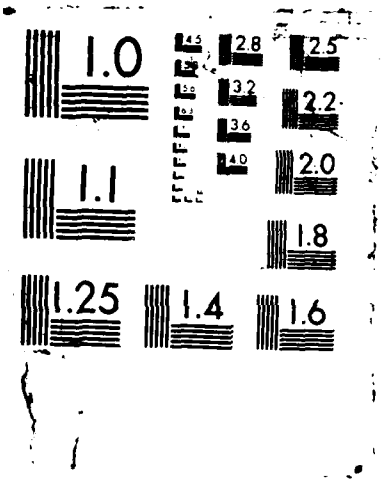
1.0
1.1
1.25
1.4
1.6
1.8
2.0
2.2
2.5
2.8
3.2
3.6
4.0
4.5

(4)

NSWC TR 87-178

AD-A191 045

CORROSION OF ELECTROLESS NICKEL-COATED STEEL

J. F. McINTYRE
S. M. HOOVER
C. M. DACRES
K. A. MUSSELMAN

RESEARCH AND TECHNOLOGY DEPARTMENT

1 APRIL 1987

NAVAL SURFACE WARFARE CENTER

Dahlgren, Virginia 22448-5000 • Silver Spring, Maryland 20903-5000

REPORT DOCUMENTATION PAGE

1a REPORT SECURITY CLASSIFICATION UNCLASSIFIED	1b RESTRICTIVE MARKINGS AD-A191043
2a SECURITY CLASSIFICATION AUTHORITY	3 DISTRIBUTION AVAILABILITY OF REPORT Approved for public release; distribution is unlimited.
2b DECLASSIFICATION DOWNGRADING SCHEDULE	
4 PERFORMING ORGANIZATION REPORT NUMBER(S) NSWC TR 87-178	5 MONITORING ORGANIZATION REPORT NUMBER(S)
6a NAME OF PERFORMING ORGANIZATION Naval Surface Weapons Center	6b OFFICE SYMBOL (If applicable) R33
6c ADDRESS (City, State, and ZIP Code) 10901 New Hampshire Avenue Silver Spring, MD 20903-5000	7a NAME OF MONITORING ORGANIZATION
8a NAME OF FUNDING SPONSORING ORGANIZATION	8b OFFICE SYMBOL (If applicable)
8c ADDRESS (City, State, and ZIP Code)	7b ADDRESS (City, State, and ZIP Code)
	9 PROCUREMENT INSTRUMENT IDENTIFICATION NUMBER
	10 SOURCE OF FUNDING NUMBERS

PROGRAM ELEMENT NO	PROJECT NO	TASK NO	WORK UNIT ACCESSION NO
64366N			

11 TITLE (Include Security Classification)
CORROSION OF ELECTROLESS NICKEL-COATED STEEL (U)

12 PERSONAL AUTHOR(S)
McIntyre, J. F. (R33), Hoover, S. M. (R32), and Dacres, C. M. (R33), K. A. Musselman (R35)

13a TYPE OF REPORT	13b TIME COVERED	14 DATE OF REPORT (Year Month Day)	15 PAGE COUNT
Technical Review	FROM 1/86 TO 5/86	1987, 04, 01	34

16 SUPPLEMENTARY NOTATION

17 COSATI CODES			18 SUBJECT TERMS (Continue on reverse if necessary and identify by block number)
FIELD	GROUP	SUB-GROUP	
11	06	01	Electroless nickel, Pitting, ~~Galvanic~~ Current, Polarization Resistance, Corrosion Resistance

19 ABSTRACT (Continue on reverse if necessary and identify by block number)

The corrosion behavior of electroless nickel-coated steel has been investigated. The effectiveness of electroless nickel as a coating is strongly dependent on the film homogeneity, thickness, and phosphorous content. Defective electroless nickel coatings are detrimental because of galvanic interaction between the coating and the steel substrate.

20 DISTRIBUTION AVAILABILITY OF ABSTRACT	21 ABSTRACT SECURITY CLASSIFICATION
☒ UNCLASSIFIED/UNLIMITED ☐ SAME AS RPT ☐ DTIC USERS	Unclassified

22a NAME OF RESPONSIBLE INDIVIDUAL	22b TELEPHONE (Include Area Code)	22c OFFICE SYMBOL
Jack F. McIntyre	(202)394-4115	R33

DD FORM 1473, 84 MAR 83 APR edition may be used until exhausted
All other editions are obsolete

SECURITY CLASSIFICATION OF THIS PAGE

☆U.S. Government Printing Office 1985-539-012

FOREWORD

Exposure of Naval ordnance and hardware to hostile environments necessitates that protective coatings be used to ensure reliability. The corrosion behavior of electroless nickel coated steel is presented in this preliminary report. Although most coatings provide adequate protection when appropriately applied, chances are that coatings will be nonhomogeneous or contain mechanical defects. Electroless nickel coatings provide good corrosion protection; however, in the presence of defects, the electroless nickel coating may actually prove to be more detrimental than beneficial. This report discusses potential corrosion problems associated with defective electroless nickel coatings used to protect mild steel.

Approved by:

JACK R. DIXON, Head
Materials Division

CONTENTS

ILLUSTRATIONS

TABLES

CHAPTER 1

INTRODUCTION

Electroless Nickel (EN) plating produces a tough coating with good corrosion resistance and wear resistance. The coating is deposited by an autocatalytic chemical reduction of nickel ions by sodium hypophosphite, a typical reaction scheme is shown below:[1]

$$H_2PO_2^- + H_2O \longrightarrow H^+ + HPO_3^{-2} + 2H_{ads} \quad (A)$$

$$Ni^{++} + 2H_{ads} \longrightarrow Ni + 2H^+ \quad (B)$$

$$H_2PO_2^- + H_{ads} \longrightarrow H_2O + OH^- + P \quad (C)$$

$$H_2PO_2^- + H_2O \longrightarrow H^+ + HPO_3^{-2} + H_2 \quad (D)$$

EN coatings are alloys of nickel and phosphorus, where their chemical and physical properties vary according to the phosphorus content. Coating thickness can range from 1.0-150 μm. The nickel-phosphorous deposit consists of a lamellar structure, with lamellae oriented parallel to the base metal[2]. X-ray analysis of the initial deposit indicates that the film structure is amorphous, i.e., glassy metal. Heat treatment of the amorphous deposit results in the formation of Ni_3P in a nickel matrix[2], which leads to an increase in the coating hardness with heat treatment up to a maximum at 400°C. However, the improved hardness and wear resistance will compromise the corrosion resistance.

A large number of metals can be EN coated, including: aluminum, beryllium, titanium, iron, nickel, copper and their alloys. To ensure a porous-free corrosion resistant coating the specimen must be free from gross defects, such as pits, crevices, scale, corrosion products and inclusions. The surface must also be clean and surface contaminants, such as, oil, grease and polishing abrasives, must be removed. In high strength steels, cracking during and after cleaning and during deposition may occur because of high internal stresses in the base metal. Severely cold-worked steels with tensile strengths greater than 1050 MPa must be stress relieved.[3] EN plating of high strength steels are usually performed using acidic surface activation solutions which can induce hydrogen embrittlement. If the surface activation process is omitted, coating adhesion is reduced; therefore, it is recommended that alkaline solutions be used for processing when ever possible.

Depending on the plating conditions, a phosphorous content of 6-12% can be achieved. At phosphorous contents below 10%, the amorphous film tends to be porous but at phosphorous levels above 10% the film is continuous.[1] Internal stresses in EN coatings are primarily a function of the phosphorous content. Coatings with more than 10% phosphorous result in a neutral or compressive surface state.[4] However, when the phosphorous content is below 10%, film stresses of 15-45 MPa are possible because of the difference in thermal expansions between the deposit and the base metal.[5] These high levels of stress can cause cracking and increase porosity of the film. A porous coating is unfavorable because of the possibility of establishing local galvanic corrosion cells. The Purpose of this investigation is to determine the effectiveness and compatibility of an electroless nickel coating to protect 1020 steel.

CHAPTER 2

CORROSION BEHAVIOR

In general, pure nickel is resistant to hot or cold alkalies, dilute nonoxidizing inorganic or organic acids and atmospheric environments. However, solutions and reagents which attack or complex pure nickel will also react with Ni-P alloys, some of these environments include: oxidizing acids, e.g., HNO_3 , oxidizing salts, e.g., $FeCl_3$, aerated NH_4OH, seawater and sulfur, at high temperatures. The corrosion resistance of pure nickel can be improved significantly when alloyed with Cu, e.g., Monel 400, Cr and Fe, e.g., Inconel 600, and Cr, Mo and Fe, e.g., Hastelloy alloys. Alloys high in phosphorus content are more resistant to attack by HNO_3 than is pure nickel.[2] Corrosion rate data for Ni-P coated steels exposed to a variety of environments is shown in Table 1. Amorphous or glassy alloys generally exhibit improved resistance over their crystalline counterparts because their structure is free from grain boundaries and grain boundary precipitates which tend to exacerbate corrosion.

EN coated steel exposed to salt-spray environments exhibits improved corrosion resistance over the steel substrate. EN also affords better protection than electrodeposited nickel.[2] A comparison between the corrosion behavior of EN and electrodeposited nickel coatings applied to steel was conducted by de Minjer and Brenner[6] and their results are summarized in Table 2. Three test exposure environments were used: exposure to the atmosphere at Kure Beach, NC (800 ft from the ocean), exposure to the atmosphere at Washington, DC and to salt-spray. Results from their tests indicated that EN coatings behaved better than electrodeposited coatings and high phosphorus contents in the coating afforded the best protection.

Although the corrosion resistance of steel is vastly improved when coated with EN, it must be realized that in order to ensure adequate protection the Ni-P coating must be homogeneous and uniform in thickness. Uneven coating thickness could lead to accelerated corrosion once thin areas of the film are breached, that is, thin spots are potential sites for pit initiation and it's highly probable that local galvanic corrosion cells will soon develop at these sites. The combined effect of pitting and galvanic interaction will lead to severe attack of the steel substrate. It is well established that an EN coating is cathodic to steel; as a consequence, the bare steel becomes the anode in the galvanic couple and preferentially corrodes. Since only small pits are formed during the initial stages of corrosion, large cathode-

TABLE 1. CORROSION RATES FOR ELECTROLESS NICKEL EXPOSED TO VARIOUS ENVIRONMENTS*

Corrosive	Time(weeks)	Aeration	MPY
Methonal	24	No	No Attack
10% Sodium Carbonate	4	No	No Attack
10% NaOH	4	No	No Attack
5% Acetic Acid	4	No	0.791
5% Acetic Acid	4	Yes	5.950
Acetone	16	No	0.003
Ammonium Hydroxide	4	No	2.300
5% Ammonium Sulfate	8	Yes	1.190
Boric Acid	8	No	0.527
5% Citric Acid	16	No	0.033
5% Critic Acid	8	Yes	0.074
HCl, pH = 1.5	4	No	1.250
HCl, pH = 1.5	4	Yes	5.320
HCl, pH = 3.5	4	No	0.074
HCl, pH = 3.5	4	Yes	0.410
72% NaOH	16	No	0.069
5% Sulfuric Acid	1	No	1.190
Deionized Water	12	Yes	0.012

* From reference (2)

TABLE 2. SUMMARY OF CORROSION RATE DATA FOR ELECTROLESS NICKEL AND ELECTRODEPOSITED NICKEL COATED STEEL*

Origin of Coating	Thickness (mils)	Kure Beach, NC Months 4	Kure Beach, NC Months 15	Wash., DC Months 14	Salt Spray Days 8
		Electroless Deposits			
Hydrac Bath	0.5	8.5	4.5	8	9
Hydrac Bath	1.0	9	9	9	9
Succinic Bath	1.0	-	9	9	5
Ammonical Bath	0.5	2	1	2	5
Ammonical Bath	1.0	3	3	2	6
Ammonical Bath	0.5	2	0	1.5	3.5
Ammonical Bath	1.0	2	2	8.5	7.5
		Electrolytic Deposits			
Ni-P, 3% P	1.0	9	5	9	4
Ni-P, 9% P	1.0	9	9	9	9
Ni, Chloride Bath	0.5	0.5	0	1	3
Ni, Chloride Bath	1.0	3	1	3	3.5

An ASTM rating is used in this table and is based on the area of the sample corroded. A rating of 10 indicates no corrosion and a rating of 0 indicates over 50% corrosion.

* From reference (2)

to-anode area ratios are formed producing large dissolution currents at the anode, i.e., bare steel. The corrosion rate of steel is accelerated leading to deep pits and/or anodic undermining of the electroless nickel coating. Therefore, a coating with good adhesion and uniform thickness is necessary to ensure good protection. In addition, as described in the introduction, the phosphorous content of the coating is another critical variable which strongly influences corrosion resistance, where approximately 10% phosphorous or more is needed to provide adequate protection.

CHAPTER 3

EXPERIMENTAL METHODS

Conventional electrochemical techniques were used to study the corrosion behavior of EN coated 1020 steel. Initial studies were conducted in 3.5% NaCl at room temperature. Sample electrodes were machined into flat disks with a diameter of approximately 1.9 cm and cold mounted in an acrylic polymer; lead wires were "crimped" into holes drilled in the specimen's side prior to cold-mounting. Prior to testing and immersion the sample's surface was degreased in acetone and methanol.

The uniform corrosion rates were determined using the polarization resistance technique, as an alternative to weight-loss measurements. This technique involves the application of a controlled-potential scan over a small range, typically ± 5mV with respect to the corrosion potential. In this potential range, the applied potential and current density are linearly related to a close approximation. A plot of the applied potential against the measured current is made. The slope of the straight line at the corrosion potential is equivalent to the polarization resistance (Rp) value, See Figure 1. The Rp value is inversely proportional to the corrosion current according to the theoretical relationship first derived by Stern and Geary[7]:

$$R_p = \Delta E / \Delta I = 1/I_{corr} \cdot (B_a \cdot B_c)/2.3(B_a + B_c) \quad (1)$$

where ΔE is the potential scan range, ΔI is the corresponding current, B_a and B_c are the anodic and cathodic Tafel constants respectively, and I_{corr} is the corrosion current. The calculated corrosion current is then used to determine the corrosion rate using the Faraday equation. A form of the Faraday equation is shown below, after some rearranging and substituting with appropriate constants:

$$MPY = 0.13 \cdot I_{corr} \cdot EW/d \cdot A \quad (2)$$

where MPY is the corrosion rate (milli-inches/year), EW is the equivalent weight in grams, I_{corr} is the corrosion current in micro-amps, d is the density in g/cc, F is the faraday constant (96,500 coulombs), and A is the surface area in cm^2.

Galvanic corrosion behavior of EN coated steel and 1020 steel was determined by using a zero-impedance ammeter to measure the generated galvanic current. Mansfeld and Kenkel[8] and Baboian[9] describe the experimental techniques which can be used to monitor galvanic corrosion currents with time. The magnitude of the galvanic current density generated for different couples is not, in

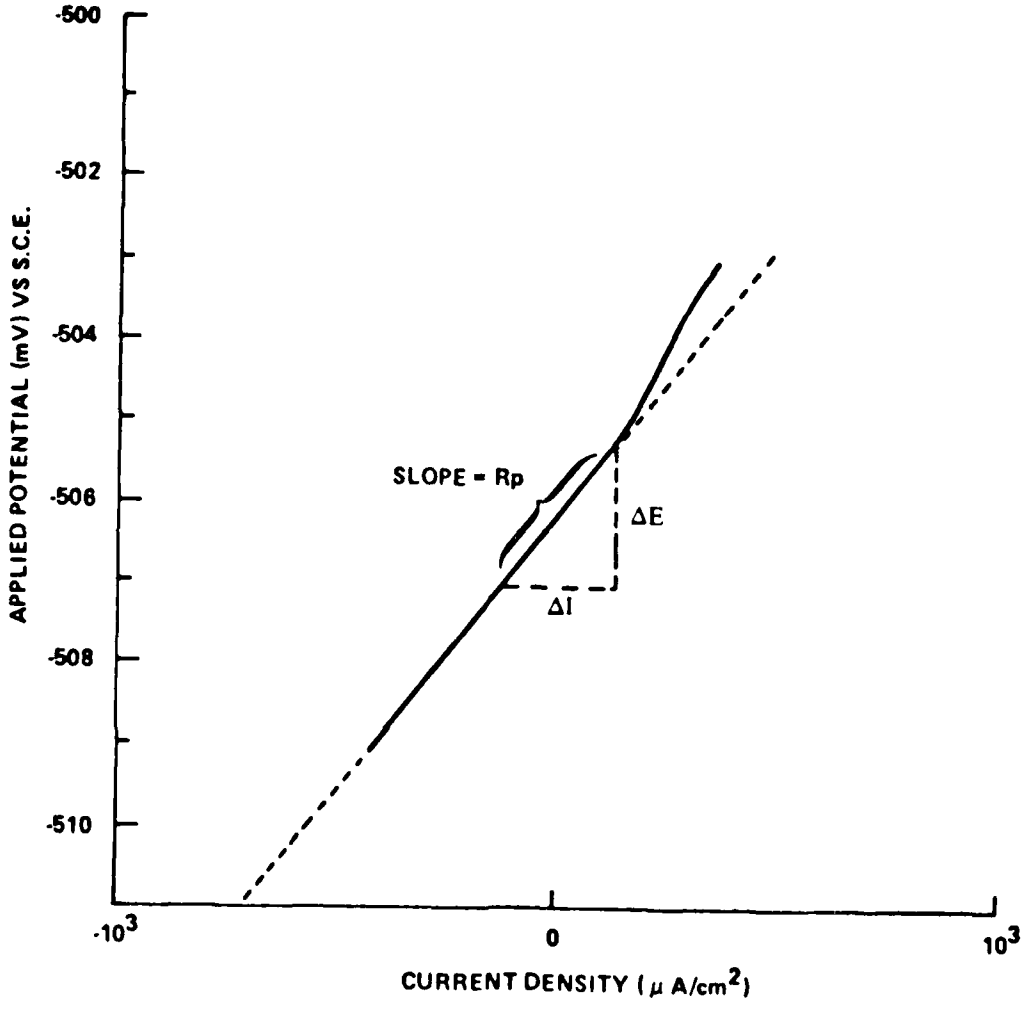

FIGURE 1. POLARIZATION RESISTANCE PLOT

most cases, directly related to the corrosion current density, i.e., corrosion rate. Mansfeld and others[10-13] present theoretical discussions on the relationships between measured galvanic currents and actual corrosion rates. For this preliminary study, two galvanic couples were tested: EN coated steel with edge defects coupled to 1020 steel and EN coated steel with a protected edge coupled to 1020 steel. All samples had approximately equal exposed surface areas.

Potentiodynamic cathodic polarization scans were conducted to obtain the limiting diffusion current density for the reduction of oxygen on 1020 steel. Scans were started at the sample's corrosion potential after stablization for one hour and scanned in the cathodic direction, i.e., negative direction, to a final value of -1.300 V (SCE).

A potentiodynamic pitting scan was obtained for an EN-steel sample with edge protection. The sample was immersed in de-aerated 3.5% NaCl and allowed to stablize for one hour before scanning. The pitting scan was started at the sample's corrosion potential, scanned in the anodic direction at a scan rate of 0.2 mV/sec and reversed at approximately 80 μA. A potentiodynamic scan typical of a metal that exhibits pitting is shown in Figure 2. The presence of a hysteresis loop usually confirms that pitting has occurred. At some potential more positive than the corrosion potential, a sample will begin to pit. This potential, E_p, is often called the breakdown potential of the metal and is determined as the potential where the measured current increases rapidly. See Figure 2. A metal's susceptibility to pitting can be determined using this technique, that is, a high positive breakdown potential or the absence of a hysteresis loop indicates that the metal is resistant to pitting.

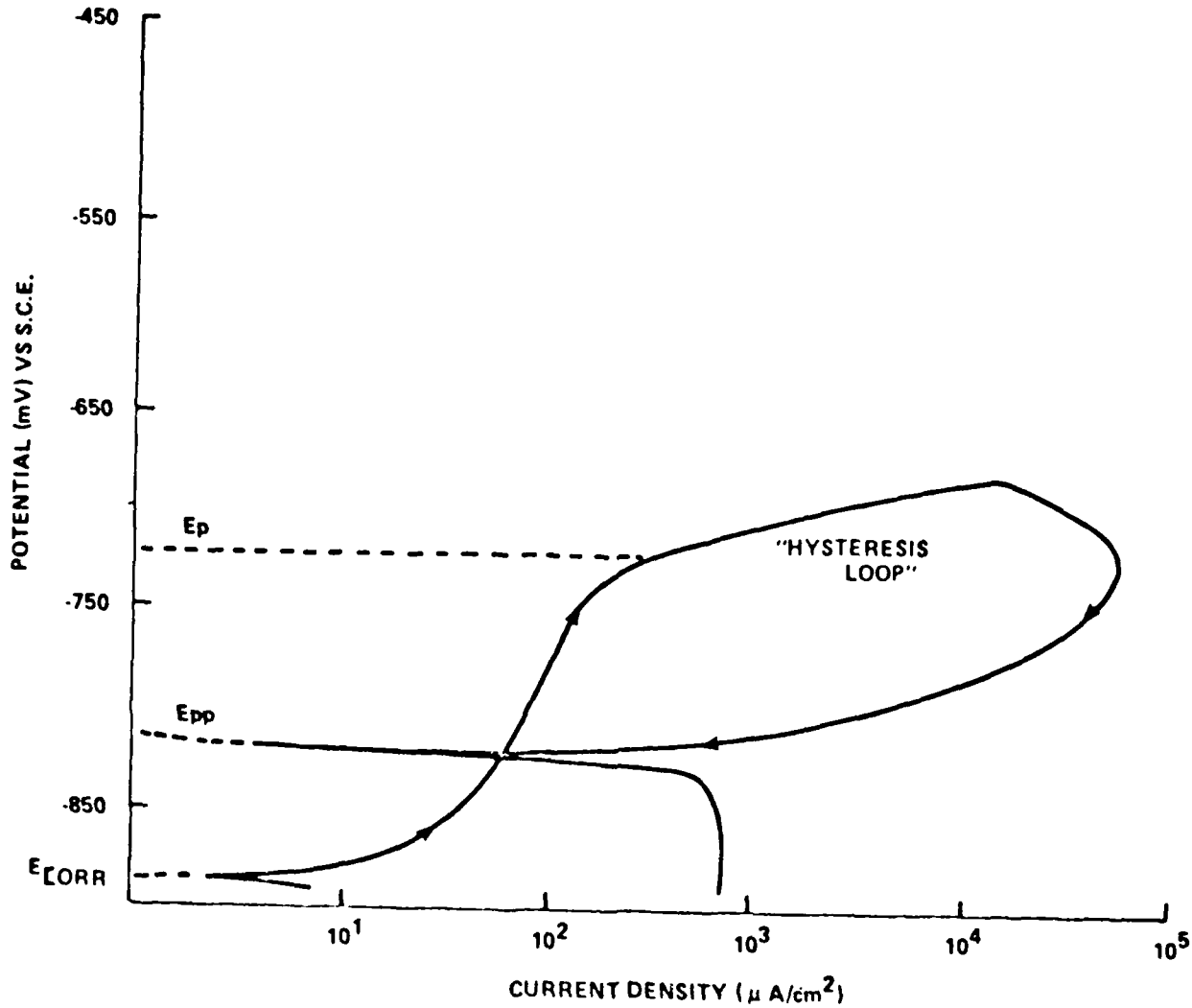

FIGURE 2. POTENTIODYNAMIC PITTING SCAN

CHAPTER 4

RESULTS AND DISCUSSION

Results reported herein are not considered to constitute a final comment on the effectiveness of the electroless nickel coating, as supplied to NSWC/WO. However, some general comments and observations can be made with confidence based on initial experimental results.

Uniform Corrosion Rates. Typical polarization resistance plots for each of the test samples are shown in Figures 3-5. It was observed that an EN sample exhibited significant edge corrosion, this localized attack was most likely due to mechanical damage introduced during the mounting process. Therefore, the edge of a subsequent EN sample was protected by the application of two coats of "glyptal" paint. A sample with a protected edge exhibited no corrosion in this area, however, at the conclusion of this test a microscopic examination revealed the EN surface was thinned in localized areas. In addition, the observed surface discoloration was due to "pinpoint" size reddish and brown spots randomly located on the surface, it was also noticed that several rust spots of relatively large diameter were present, however, no signs of pitting could be detected. A summary of the corrosion rate data is given in Table 3. As indicated in Equation (1), the corrosion current is inversely proportional to the Rp value, thus a large Rp value corresponds to a low corrosion current. The defect-free EN sample gave the highest Rp value, which was about 3.0 times greater than an EN sample with edge defects. The unprotected 1020 steel gave the lowest Rp value, as one might expect. Although it's difficult to obtain absolute corrosion rates using this technique because of the uncertainty in Tafel constant values, see Equation (1), an estimate of the corrosion rate can be obtained by using a reasonable range of Tafel values or using Tafel values selected from the literature. A modified form of Equation (1) must be used to calculate I_{corr} because this equation describes the behavior for an "activation-controlled" process; however, the corrosion rate of most metals exposed to neutral aerated NaCl are "diffusion-controlled". The following simplified equation can be used:

$$I_{corr} = 1/R_p * B_a/2.303 \qquad (3)$$

As indicated, only the anodic Tafel constant, B_a, is needed to compute I_{corr}. Once I_{corr} has been determined, the corrosion rate can be obtained from Equation (2). As a first estimate of corrosion rates, literature values were selected for B_a as shown in Table 3. For the initial estimate, the calculated corrosion rate

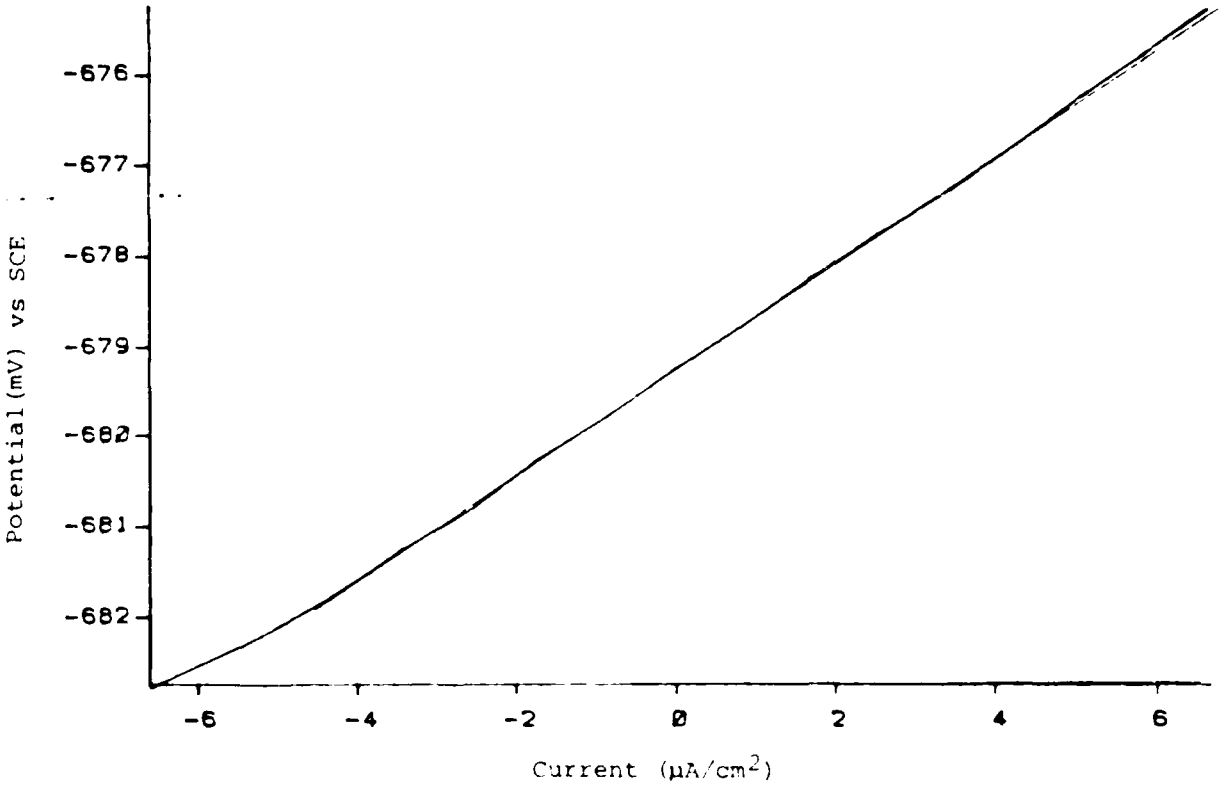

FIGURE 3. Rp PLOT FOR 1020 STEEL EXPOSED TO 3.5% NaCl

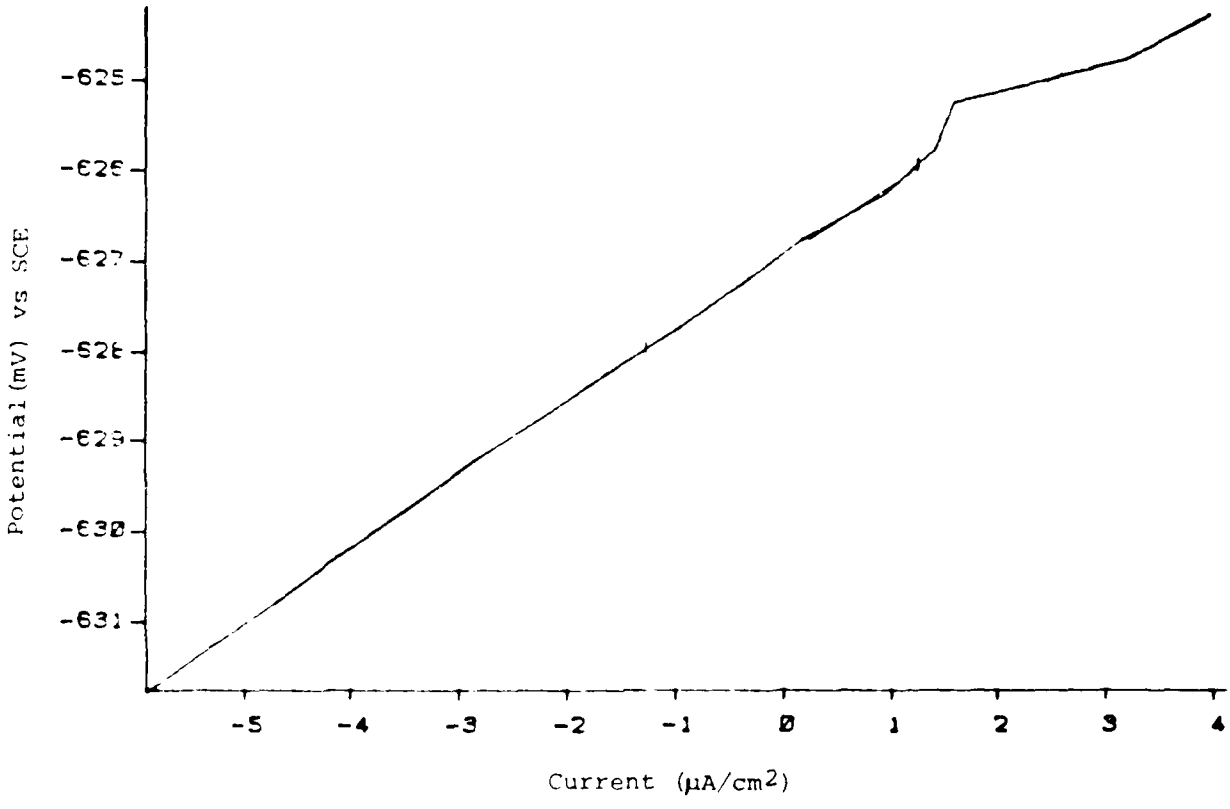

FIGURE 4. Rp PLOT FOR ELECTROLESS NICKEL COATED STEEL WITHOUT EDGE PROTECTION EXPOSED TO 3.5% NaCl

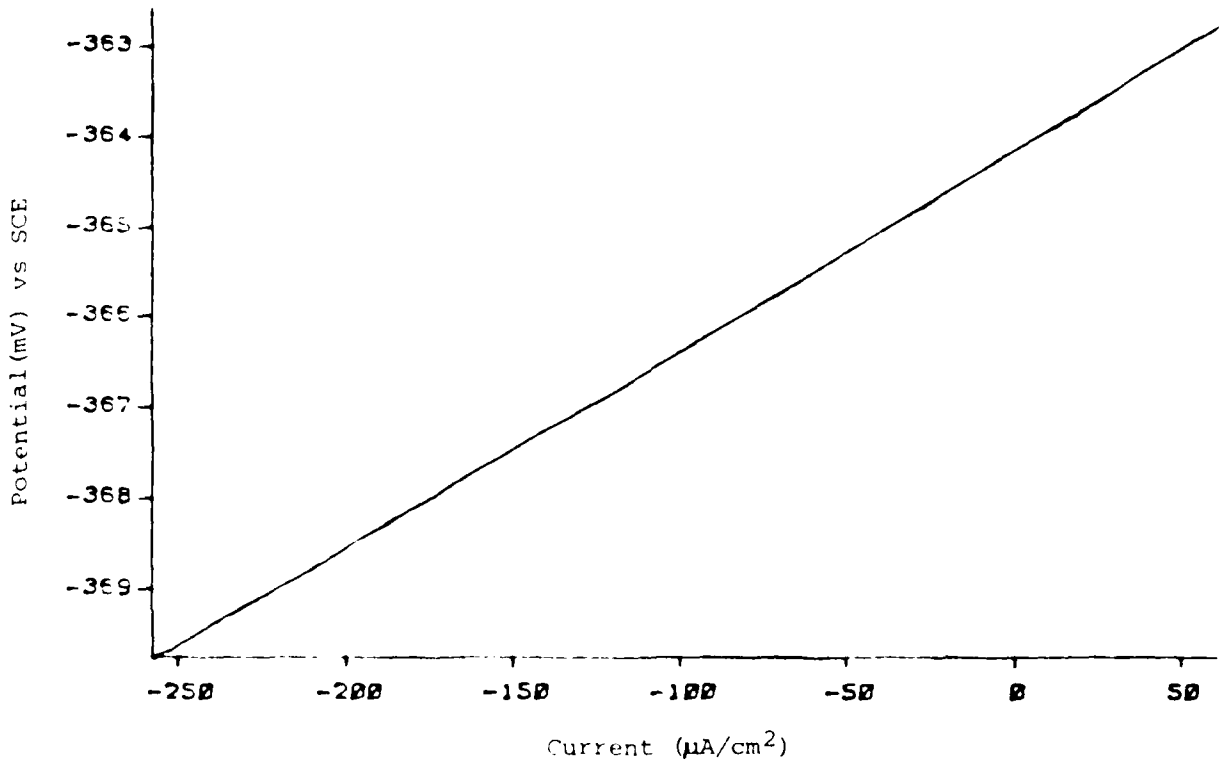

FIGURE 5. Rp PLOT FOR ELECTROLESS NICKEL COATED STEEL WITH EDGE PROTECTION EXPOSED TO 3.5% NaCl

TABLE 3. POLARIZATION RESISTANCE RESULTS FOR EXPOSURE TO 3.5% NaCl

Sample	Rp (ohms)	Literature* Icorr ($\mu A/cm^2$)	Literature* Rate (MPY)	Average Icorr ($\mu A/cm^2$)	Average Rate (MPY)
EN (Edge Coated)	2300	8.34 (95mV)	3.57	6.80	2.91
EN (Edge Uncoated)	769	18.6 (95mV)	15.1	7.95	6.48
1020 Steel	526	19.9 (70mV)	22.1	9.26	10.2

* Literature Tafel constant values are listed in parentheses.

for 1020 steel was 22.1 MPY, which was about 6 times greater than that obtained for the defect-free EN sample, 3.57 MPY. On the other hand, an EN sample with edge defects exhbited a corrosion rate of 15.1 MPY or about 4 times greater than observed for defect-free EN. As a second approximation of corrosion rates, a range of Tafel constants was selected, 55-100 mV/decade, and a mean corrosion rate was determined. Results for this approach still revealed the same trend, however, according to this method 1020 steel corroded 3.5 times faster than the defect-free sample as compared to 6 times using a literature B_a value; therefore, a corrosion rate for 1020 steel might be expected to occur between about 10.1 and 22.1 MPY or about 3-6 times faster than for defect-free EN. It's important to realize that edge defects (actual defects in this experiment constituted less than 15% of the exposed surface area) significantly reduced the effectiveness of the electroless nickel coating. This is supported by the fact that an EN sample with edge defects gave a corrosion rate which was similar to that of unprotected 1020 steel.

Galvanic Corrosion. One of the major concerns of using electroless nickel to protect steel is the strong possibility of galvanic interaction between the steel substrate and the Ni-P alloy layer. As discussed in the introduction, galvanic corrosion can be particularly insidious if a large cathode and a small anode is present. Because the corrosion rate of the anode is more or less related to the magnitude of the galvanic current, a high current distributed over a small area will produce a large current density; therefore, a small anode, a situation which could occur if the EN coating is defective or pitting corrosion has taken place, would be subjected to high currents, i.e., high corrosion rates.

Galvanic current measurements were conducted for two samples. Representative plots of measured galvanic current against measurement time are shown in Figures 6 and 7 for EN samples with and without edge defects coupled to 1020 steel. A summary of the galvanic corrosion data is given in Table 4 where galvanic currents are reported as an average galvanic current for 216 hours of immersion.

1020 steel coupled to both EN samples exhibited significant corrosion, over more than 90% of the exposed surface. The EN sample with edge defects exhibited some edge corrosion, however, the corrosion appeared to be somewhat less severe than observed for an uncoupled sample. The defect-free EN sample showed no signs of attack. As shown in Table 4, the defect-free EN/1020 steel couple gave a higher average galvanic current density than was obtained for the EN with edge defects coupled to 1020 steel. This behavior is not too surprising since an intact EN coating should act as a more efficient cathode, thus supporting higher cathodic currents which determines the magnitude of the galvanic current. The behavior of an EN coating with defects is strongly influenced by the number and size of the defects, thus significantly altering the cathodic characterisitics of the EN surface.

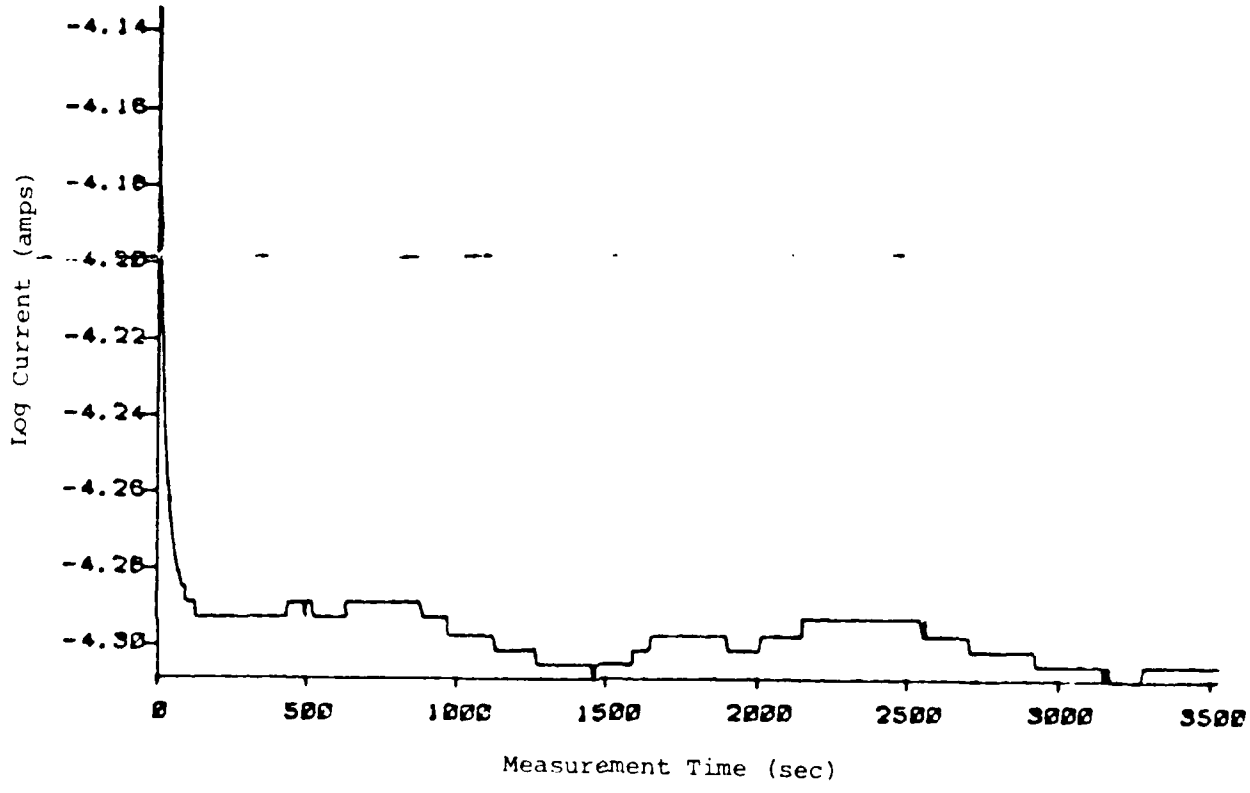

FIGURE 6. GALVANIC CURRENT PLOT FOR ELECTROLESS NICKEL COATED STEEL WITHOUT EDGE PROTECTION COUPLED TO 1020 STEEL EXPOSED TO 3.5% NaCl FOR 68 HRS

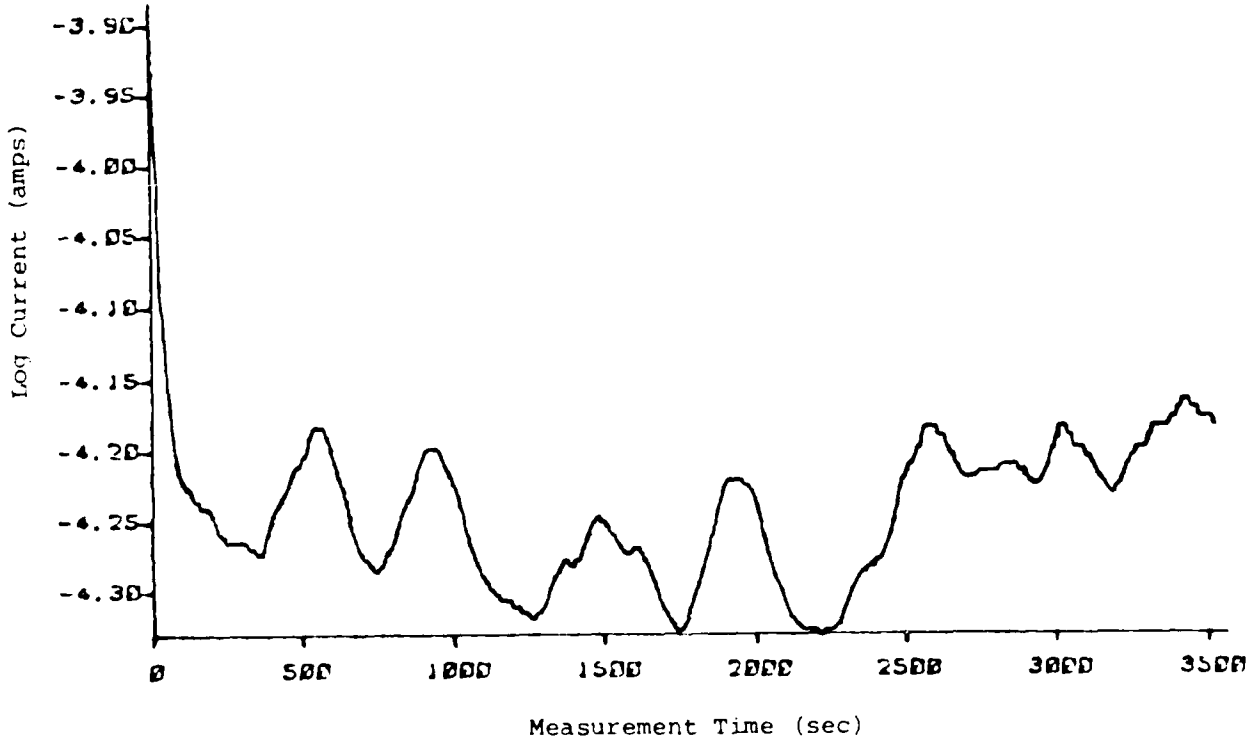

FIGURE 7. GALVANIC CURRENT PLOT FOR ELECTROLESS NICKEL COATED STEEL WITH EDGE PROTECTION COUPLED TO 1020 STEEL EXPOSED TO 3.5% NaCl FOR 96 HRS

TABLE 4. GALVANIC CURRENT RESULTS FOR EXPOSURE TO 3.5% NaCl

Couple	Ecouple (mV)	Steel-1020 Ecorr (mV)	Igal ($\mu A/cm^2$)	Corrosion Rate Steel-1020 (MPY)
EN/St-1020 (EN Edge Uncoated)	-710	-723	15.4	12.3
EN/St-1020 (EN Edge Coated)	-680	-696	20.7	15.0

Calculated corrosion rates for 1020 steel are also presented in Table 4. These corrosion rates were computed using methods outlined by Mansfeld.[10-13] It was assumed that both anodic and cathodic reactions occurred on 1020 steel for both couples, this was a reasonable assumption because the individual corrosion potentials of 1020 steel were close to the galvanic couple potential (Ecouple), See Table 4. The following equation appropriately describes this behavior:

$$i_g = i_d^a - i_{L,O_2}^a \qquad (4)$$

where the galvanic current density, i_g, is equal to the dissolution current density of the anode, i_d^a, less the cathodic current density at the anode, which is taken to be equal to the limiting diffusion current density, i_{L,O_2}^a, of the anode. The value of, i_{L,O_2}^a, was determined in a separate experiment by running a potentiodynamic cathodic polarization scan. Upon rearranging Equation (4),

$$i_d^a = i_g + i_{L,O_2}^a \qquad (5)$$

the dissolution current density of the anode (1020 steel), i_d^a, is equal to the galvanic current density, i_g, plus the limiting diffusion current density, i_{L,O_2}^a. By substituting the appropriate values into Equation (5) the corrosion rates for 1020 steel can be calculated. As seen in Table 3, the corrosion rate for uncoupled 1020 steel was between 10.1 and 22.1 MPY. Comparison of these results with those reported for coupled 1020 steel in Table 4 shows that the corrosion rate of 1020 steel increased to 12.3 MPY when coupled to EN with defects and 15 MPY when coupled to defect-free EN. This increase in the corrosion rate would be expected to increase still further when a large cathode-to-anode ratio is tested.

Pitting Corrosion. A potentiodynamic pitting scan is one method available to assess a metal's susceptibility to localized attack and results obtained for a defect-free EN sample using this technique are shown in Figure 8. A comparison between Figures 8 and 2 revealed that a typical pitting curve was not obtained for the EN sample. The shape of the curve obtained for EN revealed that no passivation region existed and no sudden rise in the pitting current occurred, thus the breakdown potential could not be determined. This type of behavior was also observed by Sorensen et al.[14] for a glassy Ni-P ribbon alloy exposed to Na_2SO_4, pH=1.5 to 11. Sorensen attributed this behavior to the existence of a nonprotective film on the Ni-P alloy which allowed dissolution to occur rapidly. Indeed, a microscopic examination of the EN sample after testing revealed that the surface was severely pitted. The pits were oriented randomly on the surface and were large in diameter, shallow, bright in appearance and no signs of corrosion product build-up was observed. Although this EN sample did not give

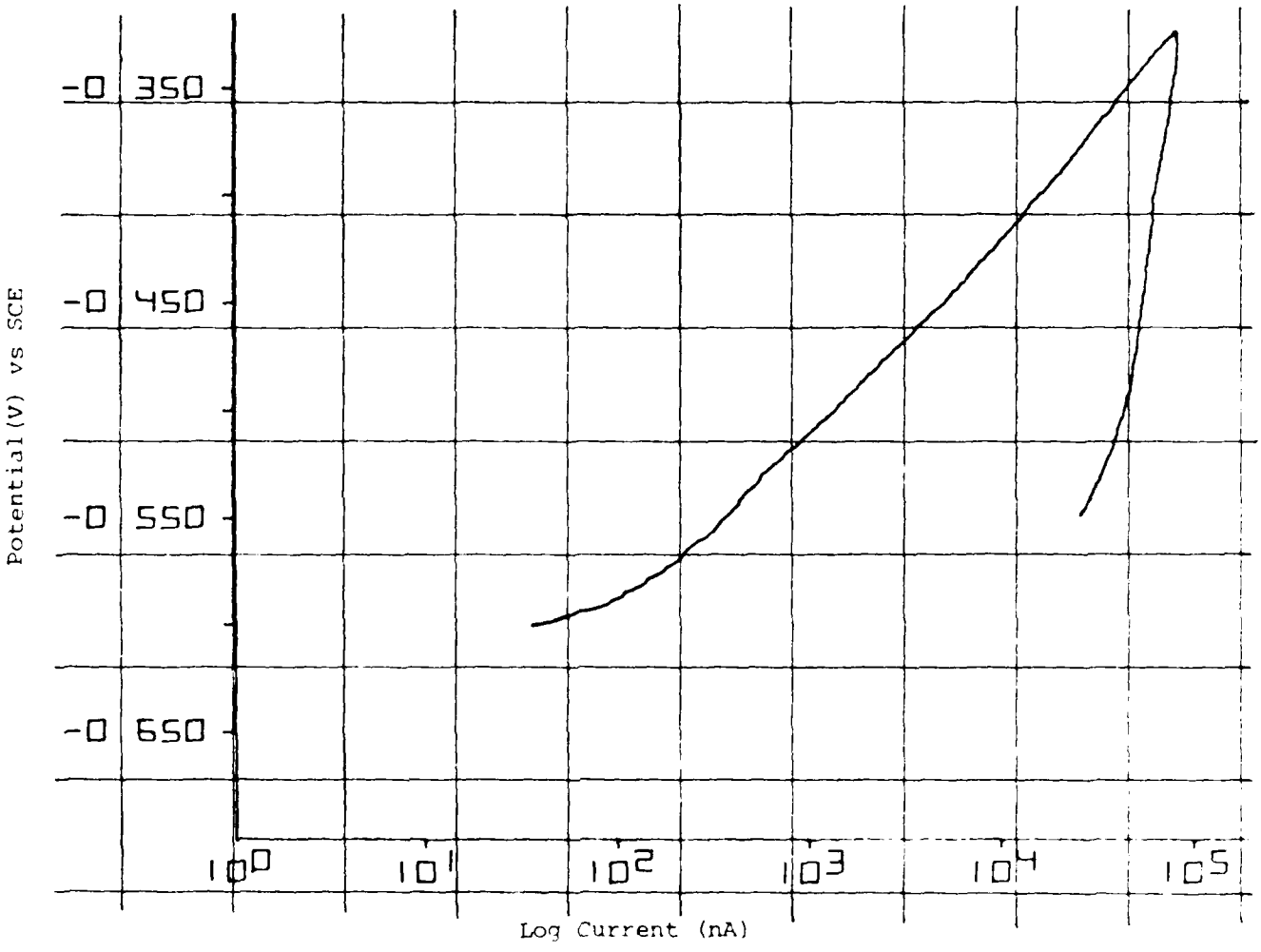

FIGURE 8. POTENTIODYNAMIC PITTING SCAN FOR ELECTROLESS NICKEL COATED STEEL EXPOSED TO DE-AERATED 3.5% NaCl

the usual pitting curve exhibited by other metals susceptible to pitting, the steady increase in current was sufficient to initiate pits, probably at low potentials.

CHAPTER 5

CONCLUSIONS

The effectiveness of electroless nickel to protect mild steel is strongly dependent on the coating's integrity. The preliminary findings reported herein demonstrated that a defective EN coating will exhibit significant corrosion. The galvanic corrosion behavior results indicated that an EN coating will be protected at the expense of the exposed steel substrate, that is, steel corrosion will be accelerated when coupled to EN. Some coating parameters which should receive attention include: phosphorous content, thickness and film homogeneity.

Future studies should involve additional studies, such as ASTM B733 Salt-Fog testing, the use of large cathode-to-anode area ratios in galvanic experiments, and immersion testing in natural seawater.

REFERENCES

1. Fields, W. D., Duncan, R. N., and Zickgraf, J. R., "Electroless Nickel Plating," Metals Handbook, 9 th Edition, 1985, p. 219.

2. "Electroless Nickel Plating," Symposium, ASTM STP 265, 1959.

3. ASTM Standards, "Autocatalytic Ni-P Deposition on Metals for Engineering Use," B656, 1984, p. 548.

4. Parker, K. and Shah, H., Plating, Vol. 58, No. 3, 1971, p. 230.

5. Duncan, R. N., Finishers Management, Vol. 26, No. 3, 1981, p. 5.

6. de Minjer, C. H. and Brenner, A., Plating, Vol. 44, No. 12, 1957, p. 1297.

7. Stern, M. and Geary, A. L., Journal of the Electrochemical Society, Vol. 104, 1957, p. 56.

8. Mansfeld, F. and Kenkel, J. V., "Galvanic and Pitting Corrosion-Field and Laboratory Studies," ED: R. Baboian, W.D. France, and J.F. Rynewicz (Philadelphia, PA: ASTM STP 576, 1976), p. 20.

9. Baboian, R., ibid., p.5.

10. Mansfeld, F., Hemgstenberg, D. H. and Kenkel, J. V., Corrosion, Vol. 30, No. 10, 1974, p. 343.

11. Mansfeld, F. and Parry, E. P., Corrosion Science, Vol. 13, 1973, p. 605.

12. Mansfeld, F., Corrosion, Vol. 29, 1973, p. 403.

13. Mansfeld, F., Corrosion, Vol. 35, No.9, 1979, p. 423.

14. Sorensen, N. R., Hunkeler, J., and Latison, R. M., Corrosion, Vol. 40, No. 11, 1984, p.619.

DISTRIBUTION

	Copies
Office of Naval Research Attn: S. Fishman, Code 1131 800 N. Quincy St. Arlington, VA 22217	2
Office of Deputy Under Secretary of Defense Attn: J. Persch Staff Specialist for Materials Washington, DC 20301	1
Defense Advanced Research Attn: P. Parrish 1400 Wilson Blvd.09 Arlington, VA 22209	1
Naval Ocean Systems Command Attn: P. D. Burke San Diego, CA 92152	1
Naval Sea Systems Command Attn: S. Rodgers, SEA 05M1 H. Bliele, SEA 05M1 Washington, D.C. 20362	1 1
Naval Air Development Center Attn: V. Agarwala, Code 6062 Warminster, PA 18974-5000	1
Naval Ship Systems Engineering Station Attn: N. Clayton Philadelphia Naval Base Philadelphia, PA 19112 Attn: N. Clayton	1
Department of the Army Attn: A. Levitt DRXMR-MMC, Bldg. 39 Watertown, MA 02712	1
Naval Research Laboratory Attn: E. McCafferty, Code 6372 P. Trzaskoma P. Natishan Washington, DC 20375	1 1 1
Naval Sea Systems Command Attn: Vance Saige PMS400C54 NC210S18 2521 Jefferson Davis Hwy Arlington, VA 22202	1
Defense Technical Information Center Cameron Station Alexandria, VA 22314	12
Library of Congress Attn: Gift and Exchange Division Washington, DC 20540	4
David Taylor Naval Ship Research and Devlopment Center Code 2813 Annapolis, MD 21402-5067	1
Naval Ship Weapon Systems Engineering Station Attn: Milton R. Scatturo Port Hueneme, CA 93043 Attn: Milton R. Scaturro	1

DISTRIBUTION (cont.)

	Copies
Naval Coastal Systems Center Attn: Jim Preston Code 3260 Panama City, FL 32407	1

Internal Distribution:		Copies
R33	(J. McIntyre)	10
R33	(R. Sutula)	1
R33	(C. Dacres)	1
R33	(Staff)	20
R30		1
R32	(S. Hoover)	1
R32	(B. Ferrando)	1
R32	(K. Vasanth)	1
R32	(J. Jarus)	1
R32	(B. Garrett)	1
R32	(J. Tydings)	1
R32	(J. Clark)	1
R35	(K. Musselman)	1
R34		1
U10	(J. Goeller)	1
U11D	(E. Johnson)	1
U13	(J. McNelia)	1
U32		1
U30		1
G20		1
G30		1
G40		1
E342	(GIDEP)	1
E231		2
E232		15
[illegible]		1

END

DATE

FILMED

5-88

DTIC